JOURNAL OF THERMOPHYSICS AND HEAT TRANSFER
Vol. 13, No. 2, April–June 1999

Performance Prediction and Control-System Design of an Aircraft Skin-Cooling Technique

Ab Hashemi,* Mary Fast,† and Julie Schneider*
Lockheed Martin Advanced Technology Center, Palo Alto, California 94304-1191
and
Elizabeth Dyson‡
Lockheed Martin Canada, Kanata, Ontario K2K 2M8, Canada

This paper describes the steady state and transient thermal response of the aft cabin of an aircraft that is retrofitted with high-power electronic equipment and cooled by heat rejection through the skin. In this skin-cooling design, the outer surface of the fuselage is treated as a heat exchanger. Hot air from an equipment exhaust plenum is drawn into a series of baffled ducts within the fuselage support structure, where heat is rejected and then recirculated into the cabin. The cooler air from the cabin is then drawn into the electronic equipment. The aircraft air-conditioning unit is also modeled to provide chilled air directly into the cabin. In addition, this paper presents an algorithm and a control-system concept to maintain the temperature of the aft cabin within acceptable limits. Results establish a control-system design, which is being implemented in a CL-600 Challenger aircraft.

Nomenclature

A	= area
c_p	= specific heat at constant pressure
c_v	= specific heat at constant volume
D_h	= hydraulic diameter
h	= heat transfer coefficient
k	= thermal conductivity
L	= length of a flat plate
M	= Mach number
m	= mass
$\dot{m}$	= mass flow rate
Nu	= Nusselt number
Pr	= Prandtl number
Q	= heat dissipation
Q_s	= solar constant
q	= heat flux
Re	= Reynolds number
s	= distance from the nose of the aircraft
T	= temperature
T^*	= recovery temperature
t	= time
U	= heat transfer coefficient
u	= velocity in the x direction
α_s	= surface solar absorptivity
ΔT	= temperature difference
ε	= surface emissivity
ξ	= beginning of heated section
ρ	= density
σ	= Stefan–Boltzmann constant

Subscripts

ACU	= air-conditioning unit
a	= ambient
aux	= auxiliary conditioned air
b	= bulk
bulkhead	= aft bulkhead
cabin	= aft cabin
ceiling	= aft cabin ceiling
e	= external
equipment	= equipment in the racks
fan	= single fan
fans	= all fans
floor	= aircraft floor
i	= internal
overall	= overall heat transfer coefficient
Racks 1, 2, 3	= electronic equipment racks
s	= local
skin	= aircraft heat-rejection surface
wi	= skin internal surface
wo	= skin external surface
∞	= far-field temperature

Introduction

TO overcome the heat-rejection limitation in a CL-600 Challenger aircraft that is retrofitted with high-power electronic equipment, a skin-cooling design has been developed.[1–4] The concept calls for baffled ducts at the aircraft skin to cool the air in the aft cabin, where the equipment is located.

The heat transfer coefficient and the pressure drop in the skin-cooling ducts were estimated using two-dimensional and three-dimensional computational fluid dynamics (CFD) models developed for this design.[1,2] These models include conjugate heat transfer and turbulence models, and consider convection and radiation exchange between the aircraft and its surroundings. The three-dimensional model predictions were verified by laboratory experiments on a representative section of the skin-cooling duct.[2] Based on analytical models and experimental data, the steady-state aft cabin temperatures for full-power operational scenarios were calculated and presented in Refs. 1 and 2.

This paper describes an analytical prediction of the steady state and transient thermal responses of the aft cabin for all mission scenarios including the effect of heat transfer to the equipment. In addition, this paper presents an algorithm and a control-system concept to maintain the temperature of the aft

Received March 13, 1998; revision received Oct. 30, 1998; accepted for publication Nov. 3, 1998.

*Missiles and Space, Thermal Sciences.
†Currently with U.S. Marine Corps.
‡Currently with Systemhouse, Hull, Quebec J8X 4B7, Canada.

cabin within acceptable limits. Results establish a control-system design, which is being implemented in the aircraft.

Configuration

A schematic of the compartments for the Challenger aircraft is shown in Fig. 1. The aircraft is split into three main areas: the cockpit, the main cabin area, and the aft cabin area, which is the location of most of the high-power electronic equipment and the skin-cooling surface area. The electronic equipment located in the aft cabin area is placed in three equipment racks. The hot air from the rack with the equipment that dissipates the most heat is exhausted into a plenum that connects to a ceiling duct, from which it is distributed by fans into the baffled ducts. These ducts, which are bounded by the cold skin on one side, are used as a heat exchanger to reject the heat to the ambient air. The cooled air is then recirculated into the aft cabin.

The baffles contained within the skin ducts increase mixing and improve overall heat transfer at the cost of increased pressure drop. In addition to the heat transfer provided by the ducts, a limited amount of chilled air is provided directly to the aft cabin from the aircraft air-conditioning unit (ACU). The specifications for each piece of equipment in the racks are summarized in Refs. 1–4.

Analysis

An analytical model was developed to calculate the aft cabin average temperature. This model is based on the principle of conservation of energy and accounts for the transient thermal response to the aft cabin. A schematic of the model is shown in Fig. 2.

In this model, the basic assumption is that heat is added to the cabin by the equipment in the racks and ceiling fans. Approximately 11 kW of heat is dissipated by Rack 1, 1 kW by Rack 2, and 2 kW by the fans. Rack 3 was assumed to be off

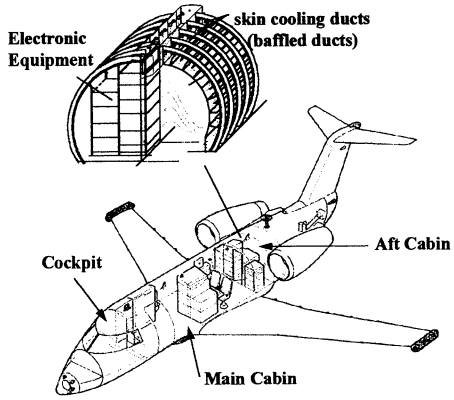

Fig. 1 Challenger cabin layout.

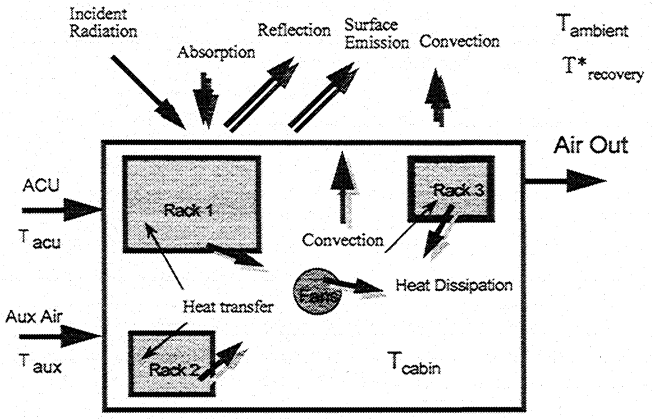

Fig. 2 Aft cabin energy balance.

for all scenarios. The ACU and auxiliary airflow effectively remove about 1 kW of heat from the aft cabin. This is ~6% of the total heat removal during full operation. The ACU and auxiliary airflow were maintained constant for all operational scenarios to avoid any complexity in the control-system design. Also, heat is transferred to the structure by convection, removed by the ACU and auxiliary airflow and rejected through the skin by convection and radiation. An overall heat transfer coefficient based on the CFD calculations[2] was used to account for the combined convection and radiation heat transfer.

The heat addition to the aft cabin may be written as

$$Q = Q_{\text{Rack1}} + Q_{\text{Rack2}} + Q_{\text{Rack3}} + Q_{\text{fans}} \tag{1}$$

Making an energy balance on the aft cabin control volume yields

$$\begin{aligned} Q = {} & \dot{m}_{\text{ACU}} c_p (T_{\text{cabin}} - T_{\text{ACU}}) + \dot{m}_{\text{aux}} c_p (T_{\text{cabin}} - T_{\text{aux}}) \\ & + m_{\text{cabin}} c_v \frac{\mathrm{d}T_{\text{cabin}}}{\mathrm{d}t} + U_{\text{overall}} A_{\text{skin}} (\bar{T}_{\text{cabin}} - T_a^*) \\ & + h_{\text{Rack1}} A_{\text{Rack1}} (T_{\text{cabin}} + \Delta T_{\text{equipment}} - T_a^*) \\ & + h_{\text{ceiling}} A_{\text{ceiling}} (T_{\text{cabin}} + \Delta T_{\text{equipment}} - T_a^*) \\ & + h_{\text{bulkhead}} A_{\text{bulkhead}} \Delta T_{\text{bulkhead}} + h_{\text{floor}} A_{\text{floor}} \Delta T_{\text{floor}} \\ & + h_{\text{equipment}} A_{\text{equipment}} (T_{\text{cabin}} - T_{\text{equipment}}) \end{aligned} \tag{2}$$

where

$$T_a^* = T_a + Pr^{1/3}(u_a^2/2c_p) = T_a\{1 + Pr^{1/3}[(\gamma - 1)/2]M^2\} \tag{3}$$

and $\bar{T}_{\text{cabin}}$ is the average heat-rejection temperature in the skin ducts, and is expressed as

$$\bar{T}_{\text{cabin}} = T_{\text{cabin}} + \tfrac{1}{2}(\Delta T_{\text{equipment}} + \Delta T_{\text{fans}}) \tag{4}$$

with $\Delta T_{\text{equipment}}$ expressing the temperature rise of the cabin air as it passes through the equipment in Rack 1:

$$\Delta T_{\text{equipment}} = Q_{\text{Rack1}}/c_p m_{\text{Rack1}} \tag{5}$$

and ΔT_{fans} denoting the temperature rise caused by heat dissipation from the fans:

$$\Delta T_{\text{fans}} = Q_{\text{fans}}/c_p m_{\text{Rack1}} \tag{6}$$

In Eq. (4), h_{Rack1} and h_{ceiling} denote the internal heat transfer coefficient on the skin in the Rack 1 and ceiling-fan plenums, respectively. In addition, h_{bulkhead} and h_{floor} designate the cabin-side heat transfer coefficient for the aft bulkhead and the cabin floor, respectively. Because these coefficients were relatively small compared with the external heat transfer coefficient, the controlling resistance to heat transfer was assumed to occur at the cabin side, and the overall heat transfer coefficient was assumed to be equal to the internal heat transfer coefficient.

For the Rack 1 plenum, the aft bulkhead, and the floor area, flow over a flat plate was assumed and the following correlation was used to calculate the heat transfer coefficient:

$$Nu = hL/k = 0.662Re^{1/2}Pr^{1/3} \tag{7}$$

For the ceiling-fan plenum, flow in a duct was assumed, and the following correlation was used to calculate the heat transfer coefficient:

$$Nu = hD_h/k = 0.023Re^{0.8}Pr^{0.33} \tag{8}$$

The equipment temperature was calculated by assuming a lumped capacitance heat transfer mechanism:

$$m_{\text{equipment}}c_{v_{\text{equipment}}}\frac{dT_{\text{equipment}}}{dt} = h_{\text{equipment}}A_{\text{equipment}}(T_{\text{cabin}} - T_{\text{equipment}}) \tag{9}$$

Equation (9) was decoupled from Eq. (2) because the thermal mass of the equipment was much larger than the cabin air. The larger thermal mass caused the thermal response of the equipment to be much longer than the cabin air.

At the outer boundary, the skin was assumed to exchange heat with the surroundings by both forced convection and radiation. For the forced convection, it was assumed that the local heat transfer coefficient could be approximated by a correlation for a flat plate with an unheated starting section[5]:

$$Nu_s = h_s s/k = 0.0296 Re_s^{0.8} Pr^{0.33}[1 - (\xi/s)^{9/10}]^{-1/9} \tag{10}$$

Averaging the local heat transfer coefficient over the heated area, the average heat transfer coefficient can be written as:

$$h_e = \int_{\xi}^{L} h_s \, ds \Big/ \int_{\xi}^{L} ds \tag{11}$$

The internal heat transfer coefficient was evaluated based on CFD calculations[2] from the following equation:

$$h_i = q/(T_b - T_{wi}) \tag{12}$$

where

$$T_b = \int \rho c_p u T \, dy \Big/ \int \rho c_p u \, dy \tag{13}$$

The overall heat transfer coefficient between the inner and outer air can then be written as

$$U = \frac{q}{(T_b - T_a^*)} = 1 \Big/ \left[\frac{1}{h_i} + \frac{\Delta y_{\text{skin}}}{k_{\text{skin}}} + \frac{T_{wo} - T_a^*}{h_e(T_{wo} - T_a^*) - \alpha_s Q_s + \varepsilon_w \sigma (T_{wo}^4 - T_\infty^4)}\right] \tag{14}$$

Estimating a value for T_{cabin} and making an energy balance on the skin,[6] an initial value for U was calculated. This U was substituted into Eq. (2) and a new T_{cabin} was obtained. The new T_{cabin} was then used in Eq. (14) to calculate a new U. This procedure was repeated until a converged solution for T_{cabin} was obtained. The effect of T_∞ was assumed negligible in the calculations.

Figure 3 shows the aft cabin average temperature for the flight envelope when all equipment are operating as a function of Mach number, i.e., speed of aircraft, flight altitude, and ambient temperature, i.e., ISA to ISA + 20°C. For example, for an aircraft flying at 25,000 ft at Mach 0.7 on an ISA + 20°C day, the predicted aft cabin temperature is ~111°F. This is the current nominal operating point and is designated with a dot on the figure. This operating point is below the maximum inlet temperature for the equipment (122°F), but above a desired design point of 105°F. The shaded regions on the graph are outside the aircraft's operating envelope. In these calculations, the ACU flow available to the aft cabin was assumed to be 6.7 lbm/min at 36°F.

Figure 3 also shows that on cold days and at high altitudes (lower edges of the flight envelope), the cabin falls below a desired temperature of 50°F (10°C). At lower operational heat loads, this problem becomes more severe. This requires a control system to maintain the aft cabin temperature within a desired range.

To maintain compatibility with the current design and to avoid major modifications and complex algorithms, it was decided to reduce the heat rejection by turning the appropriate number of fans off during cold conditions. This was recognized to control the temperature of the unoccupied aft cabin within an acceptable range (~50–110°F). The feasibility of this concept was investigated by disabling a number of recirculation fans (ceiling fans) and recalculating the steady-state cabin temperature for all operational scenarios.

Figure 4 shows the effect of turning four fans off when the cabin temperature falls below 50°F for a full-load operational scenario. This figure shows that the cabin temperature rises to within the acceptable range of (~50–110°F). The dotted arrows point to the location of the cold operating points after four fans are turned off.

Graphs similar to Fig. 4 were developed for all operational scenarios, and the appropriate number of fans were turned off to raise the aft cabin cold temperatures for each scenario. Then, various options for controlling the number of operational fans were investigated.

Initially, we explored the possibility of maintaining the aft cabin temperature by disabling a fan for every 5°F drop and enabling a fan for every 5°F increase in the aft cabin temperature. Because of the fan operation's sole dependence on the

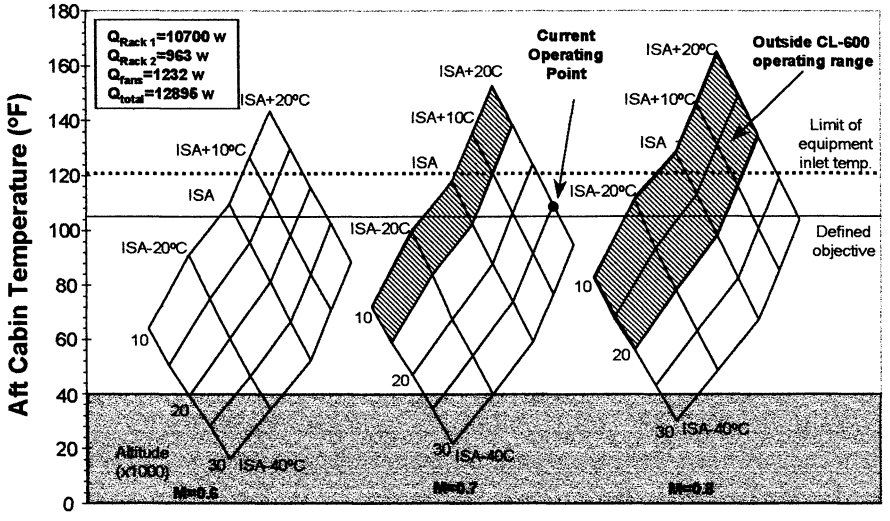

Fig. 3 Aft cabin temperature for full-load operation.

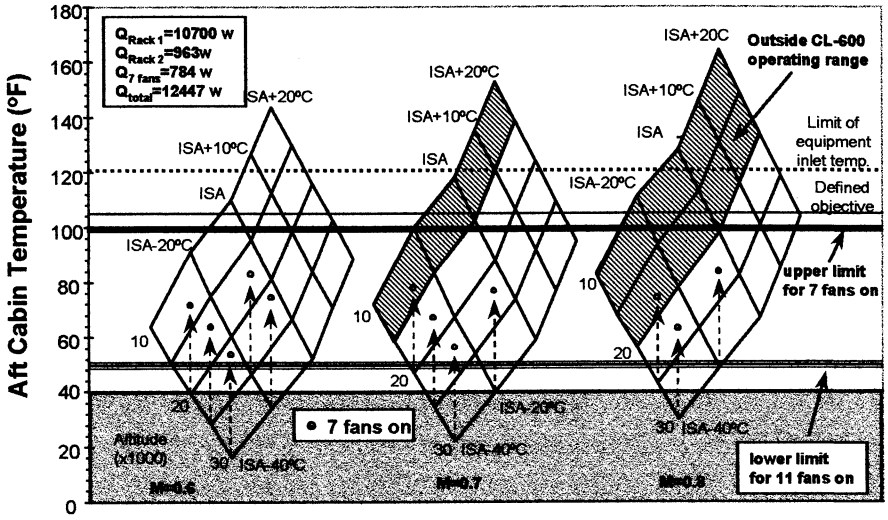

Fig. 4 Rise in aft cabin cold temperatures for full-load operation with four fans off.

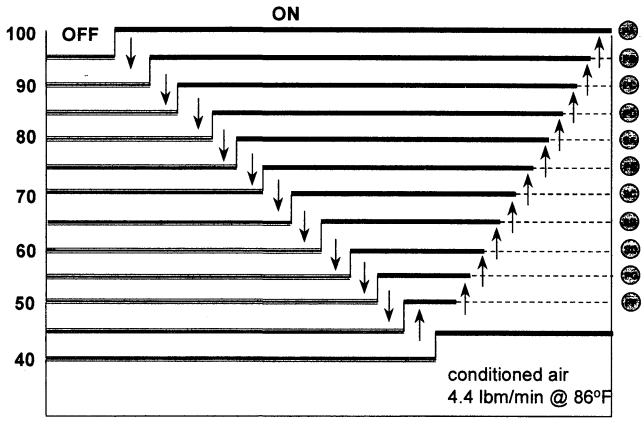

Fig. 5 Single-input, control concept for aft cabin temperature.

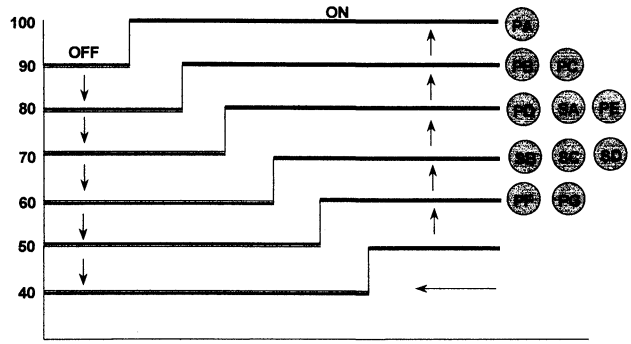

Fig. 6 Fan-cluster, single-input aft cabin temperature control concept.

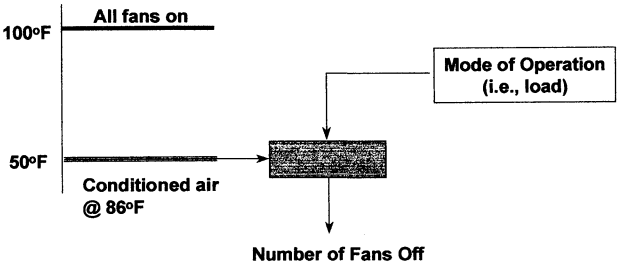

Fig. 7 Dual-input control system for aft cabin temperature.

aft cabin temperature, this technique was designated as the single-input control concept. Figure 5 shows a schematic of the single-input control concept. For every 5°F drop in cabin temperature, a fan is turned off, and for every 5°F increase in cabin temperature, a fan is turned on. The circled letters on the right, i.e., PA, PB, etc., designate a specific fan in the system. The conditioned airflow (4 lbm/min at 86°F) introduced into the aft cabin was assumed unchanged for all of the scenarios. This is a result of a practical limitation in the existing system and its minimal impact for most of the scenarios.

The single-input aft cabin temperature control caused a very fast and impractical hysterics of the fans as a result of rapid changes in the operational load and the small size of the aft cabin. The next attempt in designing the control system was to cluster the fans in a group and couple their operation to the aft cabin temperature. This was deemed to provide us with a wider hysterics band, and thus, less switching of the fans. This concept is shown in Fig. 6. The margin for deactivation and activation of the fans was increased to 10°F. But, again, this concept caused unacceptable hysterics of the fans and was ruled out.

Finally, a dual-input control system for the aft cabin temperature was considered. This concept is shown in Fig. 7. The dual-input control system is based on anticipating the steady-state temperature by detecting the load and then disabling appropriate number of fans as the cabin temperature falls below 50°F. When the cabin temperature reaches 100°F, all 11 fans are turned on. In this design, the temperature of the unoccupied aft cabin is allowed to reach a steady-state value within a wide margin (~500–100°F), and yet tolerate rapid changes in the heating load.

To implement the dual-input design, an estimate of the number of disabled fans as a function of heat load is required. This was accomplished by estimating the number of fans required to maintain the aft cabin temperature within the acceptable range for all operational scenarios for cold conditions. Figure 8 shows the number of operating fans required to maintain the aft cabin temperature between 50°F and 110°F. The arrows in the figure point to heat loads corresponding to specific equipment operation.

To estimate the aft cabin temperature for off-design conditions, each operational scenario was re-examined by disabling more than the optimum number of fans for that scenario. This provided us with a prediction of an acceptable margin for the number of fans for each scenario. Figure 9 shows the effect of disabling five fans on the aft cabin temperature for a full

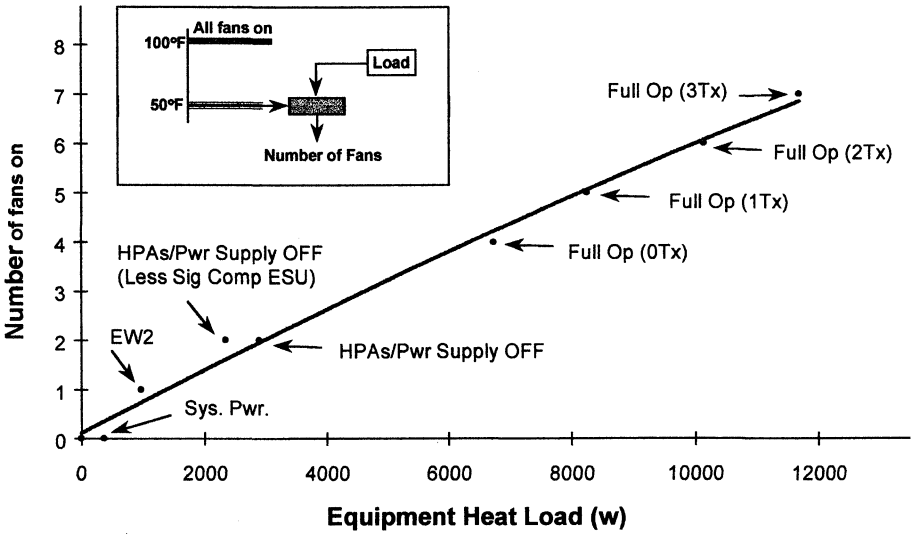

Fig. 8 Number of operating fans as a function of heat load for cold condition.

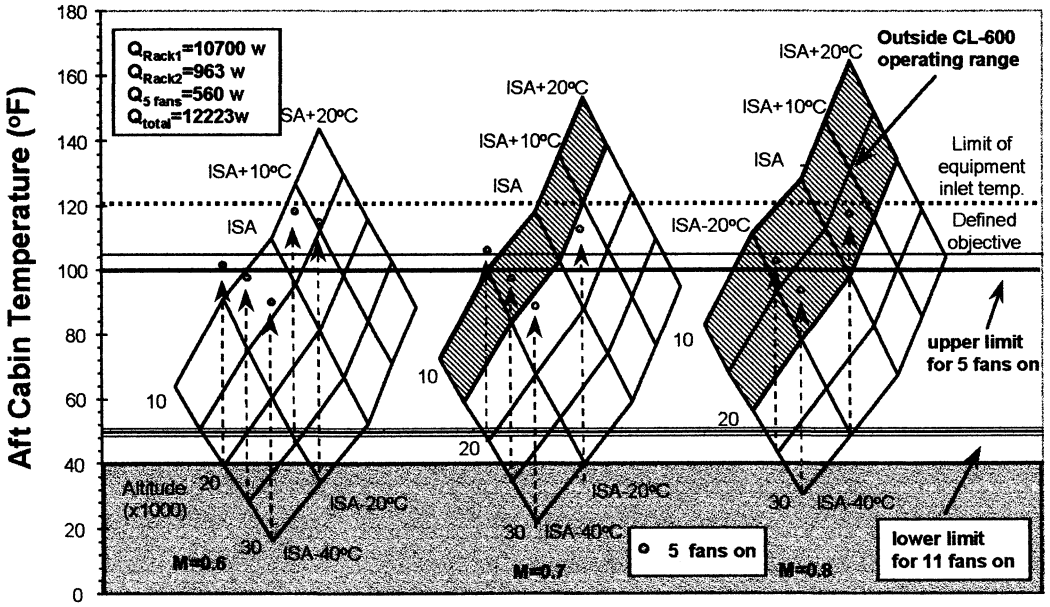

Fig. 9 Rise in aft cabin cold temperatures for full-load operation with seven fans off.

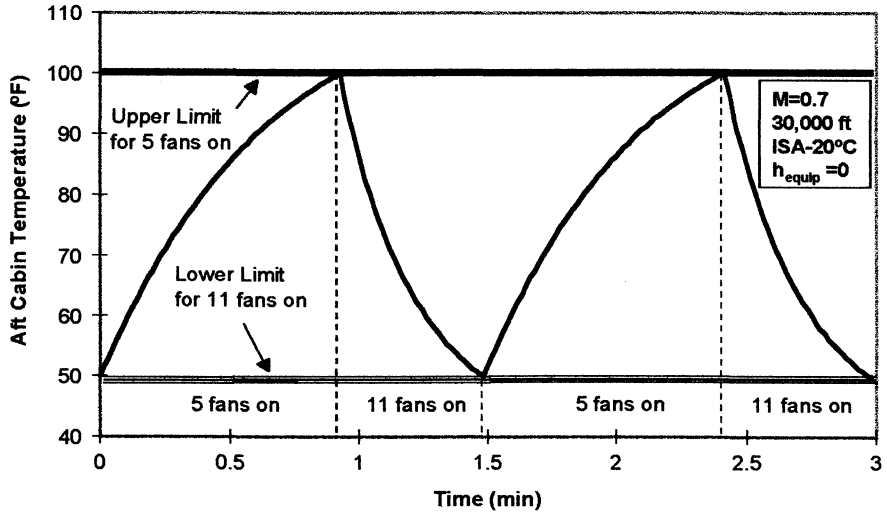

Fig. 10 Aft cabin transient temperature for full-load operation with five fans on for cold conditions.

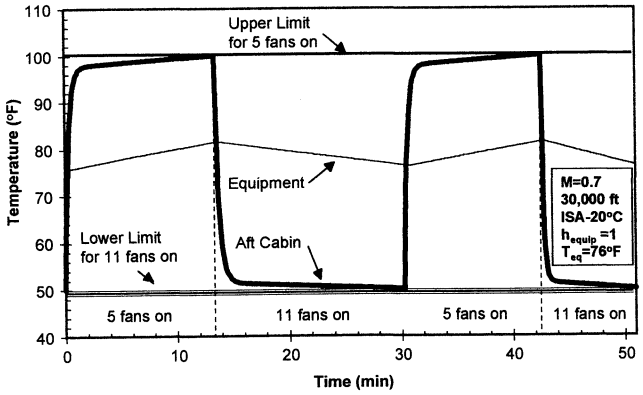

Fig. 11 Effect of heat transfer to equipment on aft cabin transient temperature for full-load operation with five fans on for cold conditions (equipment initial temperature = 76°F).

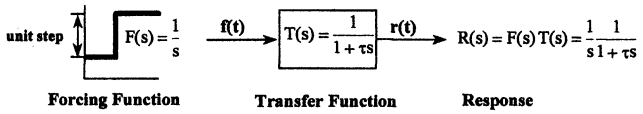

$$r(t) = L^{-1}\{R(s)\} = L^{-1}\{F(s)\,T(s)\} = L^{-1}\left\{\frac{1}{s}\,\frac{1}{1+\tau s}\right\} = 1 - e^{-\frac{t}{\tau}}$$

Fig. 12 Rolloff filter formulation.

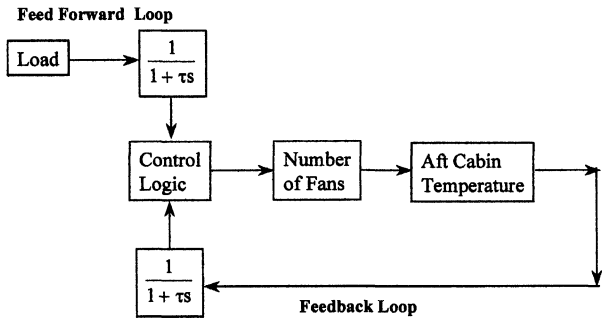

Fig. 13 Fan control-system block diagram.

load during cold conditions. For this condition, the steady-state aft cabin temperature reaches unacceptably high values (>110°F).

Because the time to reach steady state is the critical parameter in the performance of the control system, the transient behavior of the aft cabin temperature for the preceding condition, i.e., five fans on, full operation, cold conditions, was investigated. Results are shown in Fig. 10.

Figure 10 shows that for this scenario, five fans turn on and off every 1.5 min. Although this is perhaps acceptable for operational purposes, a closer examination of the control algorithm shows that the time constant is much longer than 1.5 min.

To predict a realistic estimate of the aft cabin transient temperature, the effect of heat transfer to structures was included in the analysis. The transient response of the aft cabin temperature, accounting for the heat transfer to the equipment, is shown in Fig. 11. The time constant for tripping the fans was increased to about 13 min (compared with 1.5 min for no equipment heat transfer). For this calculation, the initial temperature of the equipment was assumed to be 76°F. However, a wide range of initial temperatures was examined. Other than the first cycle, no noticeable difference was observed in the time constant. Similar calculations were carried out for all operational scenarios.

The coefficient for heat transfer to the equipment was assumed to be 1 Btu/h-ft^2-°R. Performing a test in a room roughly the size of the aft cabin with several cabinets inside the room validated this value. Three, 1-kW heaters were used to simulate the heat load. The room temperature was measured using a chromel–constanten thermocouple, and the results were compared with predictions using a heat transfer coefficient of 1 Btu/h-ft^2-°R for all of the surfaces in the room.

To allow more flexibility in the control system, two rolloff filters were included in the dual-input control concept. The mathematical formulation of the filters is shown in Fig. 12. This formulation is based on a basic Laplace transform that can be found in most control theory textbooks.

A block diagram of the control system with filters is shown in Fig. 13. The basic concept calls for a flexibility to dampen the feed-forward loop and/or the feedback loop. For completeness, the response of the system to a step-input for the various rolloff time constants is shown in Fig. 14. Other inputs were also examined and the flexibility in the design was verified.

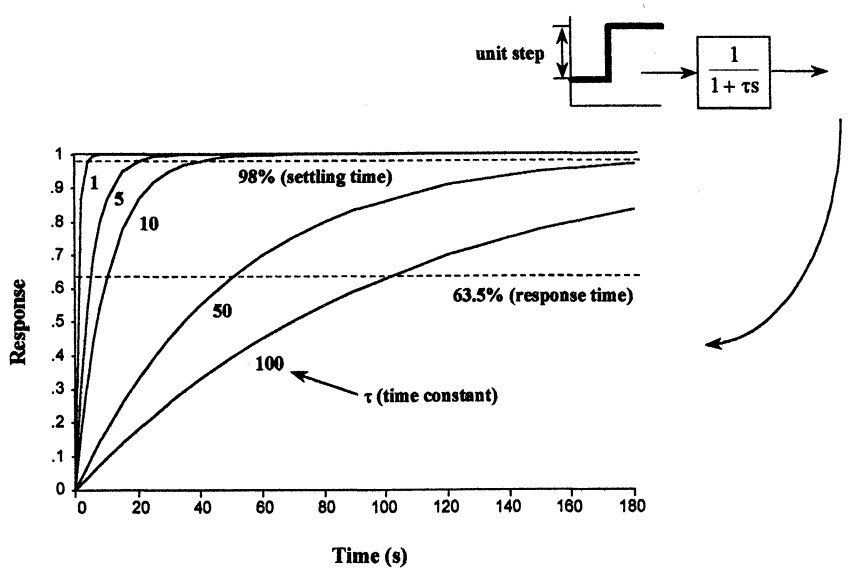

Fig. 14 Time constant.

Conclusions

The performance of a supplementary skin-cooling concept for an aircraft with onboard high-power electronic equipment has been analytically characterized for the entire mission envelope. Using the current design parameters, the aft cabin temperature falls below 50°F (~10°C) for many operational scenarios. To maintain the unoccupied aft cabin temperature within an acceptable range (50–110°F), several control concepts were considered.

A single-input control system that is based on disabling an appropriate number of recirculating fans as a function of temperature drop in the aft cabin was ruled out because of a potentially rapid switching requirement for the fans. This control concept requires very accurate and fast-responding temperature sensors and a more sophisticated design approach to overcome system transients.

A dual-input control system was developed in which the steady-state aft cabin temperature is estimated based on the heat load in the aft cabin and the switching of appropriate number of fans is accomplished at a set cabin temperature. The control logic is based on anticipating the aft cabin thermal load by measuring the input power (feed-forward loop) and measuring the resultant temperature (feedback loop). Currently, the set points are 50°F for disabling the fans when the temperature is decreasing and 100°F for enabling all of the fans when the temperature is increasing. Sufficient flexibility is designed into the system to adjust the set points during the implementation of the design. Two rolloff filters in the control system are also designed to damp out the load and temperature fluctuations and to prevent excessive fan modulations.

An additional control algorithm has been designed for ground operation, takeoff, ferry, and landing, i.e., high skin temperature override, supply of conditioned air, etc.

References

[1]Hashemi, A., Dyson, E., and Wong, H., "Cooling of Onboard High-Power Electronics Using Augmented Heat Rejection from Aircraft Skin," *Proceedings of the Symposium on Thermal Science and Engineering in Honor of Chancellor Chang-Lin Tien* (Berkeley, CA), 1995, pp. 465–474.

[2]Dyson, E., Hashemi, A., and Wong, H., "High-Power Electronics Heat Rejection from Aircraft Skin," *Journal of Enhanced Heat Transfer*, Vol. 3, No. 3, 1996, pp. 165–176.

[3]Hashemi, A., and Dyson, E., "Design of an Aircraft Skin Cooling System for Thermal Management of Onboard High Power Electronic Equipment," *Proceedings of the ASME 31st National Heat Transfer Conference* (Houston, TX), Vol. 7, 1996, pp. 233–243.

[4]Hashemi, A., and Dyson, E., "Performance Characterization of High-Power Electronic Equipment Onboard an Aircraft," AIAA Paper 97-0596, Jan. 1997.

[5]Incropera, F. P., and Dewitt, D. P., *Fundamentals of Heat and Mass Transfer*, 3rd ed., Wiley, New York, 1990.

[6]Hashemi, A., Wong, H., Schneider, J., and Dyson, E., "Skin Thermal Response for an Aircraft with Supplementary Skin Cooling System," AIAA Paper 98-0838, Jan. 1998.